DOI: 10.1002/ejic.200601014

Spin Canting and Topological Ferrimagnetism in Two Manganese(II) Coordination Polymers Generated by In Situ Solvothermal Ligand Reactions

Lin Cheng,[a] Wei-Xiong Zhang,[a] Bao-Hui Ye,*[a] Jian-Bin Lin,[a] and Xiao-Ming Chen*[a]

Keywords: Solvothermal ligand reaction / Coordination polymers / Spin canting / Topological ferrimagnetism

Two manganese(II) coordination polymers, $[Mn_2(bpt)(pa)_2(N_3)]_n$ [**1**; Hpa = picolinic acid, Hbpt = 3,5-bis(2-pyridyl)-4*H*-1,2,4-triazole] and $[Mn_3(ina)_2(pa)_2(N_3)_2]_n$ (**2**; Hina = isonicotinic acid), have been synthesized by solvothermal treatment, in which the ligands bpt and pa were generated in situ by cyclocondensation and hydrolysis of 2-pyridylamidrazone, respectively. In **1**, each binuclear subunit $[Mn_2(bpt)(N_3)]$ bridged by bpt and N_3^- ligands is interlinked to four adjacent subunits via four tridentate pa ligands into a diamondoid 3D network, which shows spin-canting magnetism arising from the lack of inversion centers between the interacting spin centers. In **2**, the Mn^{II} ions are alternately connected by double $\mu_{1,3}$-carboxylate/$\mu_{1,1}$-azide and double $\mu_{1,1}$-carboxylate bridges into a 1D magnetic chain, which exhibits a topological ferrimagnetic behavior in an antiferromagnetic-antiferromagnetic-ferromagnetic sequence. These chains are further interlinked via ina ligands into a 2D network.

Introduction

Recent years have witnessed an explosion of interest in molecular-based magnetic materials, since such materials can help in understanding magneto-structural correlations and some fundamental phenomena of magnetism, and may have potential applications.[1–4] A basic design route for this kind of magnetic materials is to appropriately organize the paramagnetic ions into ordered polynuclear architectures by use of bridging ligands that can efficiently transmit magnetic superexchange. In addition to the nature of the metal centers, the bulk magnetic properties mainly depend on the bridging modes and bridging geometries of the bridging ligands. This fact provides an opportunity to produce new molecule-based magnetic materials by crystal engineering, although so far the pursuit of designing polynuclear complexes and extended networks with predictable magnetic properties is still a challenge, because the structural factors governing the exchange coupling between paramagnetic centers are complex and elusive. Azide was widely used to connect metal ions, and the correlation between the structure and magnetic properties of the end-on (EO), or $\mu_{1,1}$-azide, and end-to-end (EE), or $\mu_{1,3}$-azide, coordination modes was observed, generally giving ferro- (F) and antiferromagnetic (AF) interactions, respectively. The interactions also depend highly on the M–N–M angle;[5,6] however, these angles are mutable and difficult to predict and control in the uniquely azide-bridged complexes. Therefore, the introduction of a second bridging ligand to control the exchange angle between the metal ions may provide a feasible approach to the construction of bulk magnetic materials. Furthermore, multidentate ligands containing a carboxylate and a pyridyl group, such as nicotinate (na), isonicotinate (ina), and picolinate (pa), have been frequently used in the preparation of magnetic materials, because the various coordination modes adopted by the carboxylate group can transmit the magnetic coupling in different degrees, and the coordination of the pyridyl and carboxylate groups in these ligands may result in extended frameworks.[7] Unfortunately, the examples of higher dimensional (2D and 3D) molecule-based magnetic materials in which bridging azide and carboxylate groups coexist are relatively rare so far.[8]

Meanwhile, the hydro(solvo)thermal technique has been successfully applied to synthesize inorganic materials,[9] inorganic–organic hybrid materials, and coordination polymers.[10] It facilitates not only the assembly and crystallization of functional metal coordination polymers that can not be directly assembled from the organic ligands and metal ions,[10] but also some important in situ ligand reactions,[11–13] leading to the formation of in situ generated mixed-ligand coordination polymers that can not be easily obtained otherwise.[13f]

During our study of the reaction mechanisms of different organonitriles with hydrazine hydrate,[14] two new mixed-ligand polymeric manganese(II) complexes, $[Mn_2(bpt)(pa)_2(N_3)]_n$ [**1**; Hpa = picolinic acid, Hbpt = 3,5-bis(2-pyridyl)-4*H*-1,2,4-triazole] and $[Mn_3(ina)_2(pa)_2(N_3)_2]_n$ (**2**; Hina =

[a] MOE Key Laboratory of Bioinorganic and Synthetic Chemistry, School of Chemistry and Chemical Engineering, Sun Yat-Sen University,
Guangzhou 510275, China
Fax: +86-20-8411-2245
E-mail: cesybh@mail.sysu.edu.cn
cxm@mail.sysu.edu.cn

Supporting information for this article is available on the WWW under http://www.eurjic.org or from the author.

isonicotinic acid), containing azide and carboxylate bridges, have been synthesized and characterized by single-crystal X-ray diffraction and low-temperature magnetic studies.

Results and Discussion

Synthesis

Compound **1** was synthesized under solvothermal conditions with 2-pyridylamidrazone and azide anion in the presence of Mn^{II} salt, in which both bpt and pa ligands were generated in situ (Scheme 1). Interestingly, bpt was obtained by the cyclocondensation reaction of 2-pyridylamidrazone in the presence of Mn^{II} ion.[14] Meanwhile, the hydrolysis reaction was also observed. It is not surprising to observe the hydrolysis reaction of 2-pyridylamidrazone to pa at high temperature and pressure, since amidrazone groups can be hydrolyzed to carboxylate groups under common reaction conditions.[15] Presumably, Mn^{II} ions promote the hydrolysis of 2-pyridylamidrazone.[16] When $Mn(ina)_2$ salt was used in place of $MnC_2O_4{\cdot}3H_2O$, **2** was produced, and only the hydrolysis but not the cyclocondensation reaction was observed. This fact may be attributed to the different Mn^{II} sources, as the structure of the 3D $Mn(ina)_2{\cdot}0.5EtOH{\cdot}0.5H_2O$ is more stable than that of the 1D $MnC_2O_4{\cdot}3H_2O$.[17,18] Obviously, it is more difficult to release Mn^{II} ions, which can facilitate cyclocondensation reactions, from the more stable Mn^{II} salt.

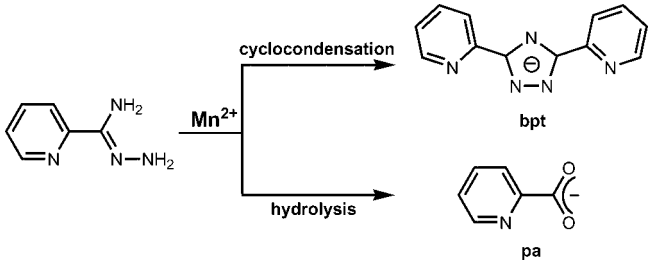

Scheme 1. The in situ solvothermal ligand reaction of 2-pyridylamidrazone in the presence of Mn^{II}.

Description of the Crystal Structures

[Mn$_2$(bpt)(pa)$_2$(N$_3$)]$_n$ (1)

Compound **1** crystallizes in the acentric *Fdd*2 space group. Each bpt ligand binds to two Mn^{II} ions [Mn1–N1 2.301(4) and Mn1–N2 2.222(4) Å] in a *cis* bis(chelate) mode. A pair of Mn^{II} ions are additionally bridged by an azide ligand in the EE mode [Mn1–N5 2.198(4) Å] and further coordinated by four pa ligands derived from the hydrolysis of 2-pyridylamidrazone to furnish a dinuclear secondary building unit (SBU) (Figure 1a). The intradimer distance Mn1···Mn1A is 4.665 Å, much shorter than that in the dinuclear Mn^{II} complexes double bridged by EE azide (5.166–5.485 Å).[5c,19] Furthermore, each SBU connects four adjacent SBUs via the μ-carboxylate bridges of four pa ligands into a 3D coordination polymer (Figure 1b), in which each pa acts as a tridentate ligand and each carboxylate group bridges two SBUs in a *syn-anti* coordination mode (Mn···Mn 6.080 Å). From the topological point of view, each SBU can be considered as a four-connecting node, which is connected by four bridging pa ligands as two-connecting linkers. Consequently, the 3D network can be regarded as a diamondoid structure, as shown in Figure 1c.

[Mn$_3$(ina)$_2$(pa)$_2$(N$_3$)$_2$]$_n$ (2)

Compound **2** is a 2D coordination polymer constructed by trinuclear SBUs with the bridging ligands ina, pa, and N_3^-. There are two crystallographically independent Mn^{II} ions in each SBU (Figure 2a), in which Mn1 is located at a crystallographic inversion center and displays a slightly distorted octahedral geometry, being surrounded by four oxygen atoms [Mn1–O4 2.125(2) and Mn1–O2A 2.207(1) Å] from two pa and two ina ligands as well as by two nitrogen atoms [Mn1–N3 2.227(2) Å] from two N_3^-. On the other hand, the Mn2 atom adopts an N_3O_3 geometry, being coordinated by a chelating pa ligand [Mn2–N1 2.257(2), Mn2–O1 2.216(2) Å], one bridging oxygen atom from another pa, and a nitrogen atom of one EO azide [Mn2–N3 2.134(2) Å] ligand, as well as one oxygen and one nitrogen atom from two ina ligands [Mn2–N2d 2.357(2), Mn2–O3 2.168(1) Å]. The coordination modes of ina, pa, and azide in **2** are depicted in Figure 3. The Mn1 and Mn2 atoms are bridged by two *syn-syn* μ-1,3-carboxylate groups of the ina and pa ligands as well as by an EO azide ligand. Furthermore, the SBUs are interlinked to each other via two single oxygen bridges to form a chain. The Mn1···Mn2 distance is 3.569 Å, being markedly shorter than that of a mixed-ligand Mn^{II} complex featuring a *syn-syn* carboxylate and an EO azide (3.861 Å) ligand.[8c] The Mn1–N3–Mn2 angle [109.86(8)°] is significantly larger than the crossover angle between AF and F interactions on the EO coordination mode of azide[5a] and the experimental observations (100.5–104.1°),[5c,19] but much smaller than that reported in $[Mn_3(N_3)_2(na)_4(H_2O)_2]$ (118.6°).[8c] The Mn2···Mn2A distance is 3.512 Å, comparable with those in carboxylate-bridged trinuclear Mn^{II} complexes,[20] and the Mn2–O1–Mn2A angle is 105.56(6)°. The adjacent chains are further linked by tridentate ina ligands (Figure 3a) into a 2D network. The interchain Mn···Mn distances across the ina ligands are 9.073 and 9.527 Å.

Magnetic Properties

Magnetic Properties of 1

The magnetic susceptibility of powder **1** was investigated in the temperature range 2–300 K at an applied field of 500 G, and the plots of χ_M and $\chi_M T$ vs. T are shown in Figure 4. When the sample is cooled from 300 K, the χ_M per Mn^{II} exhibits a smooth increase to a rounded maximum of 0.038 emu mol^{-1} at ca. 25 K, then decreases slightly to 0.037 emu mol^{-1} at 7.8 K, and thereafter increases rapidly to 0.110 emu mol^{-1} at 2 K. Meanwhile, the $\chi_M T$ per Mn^{II}

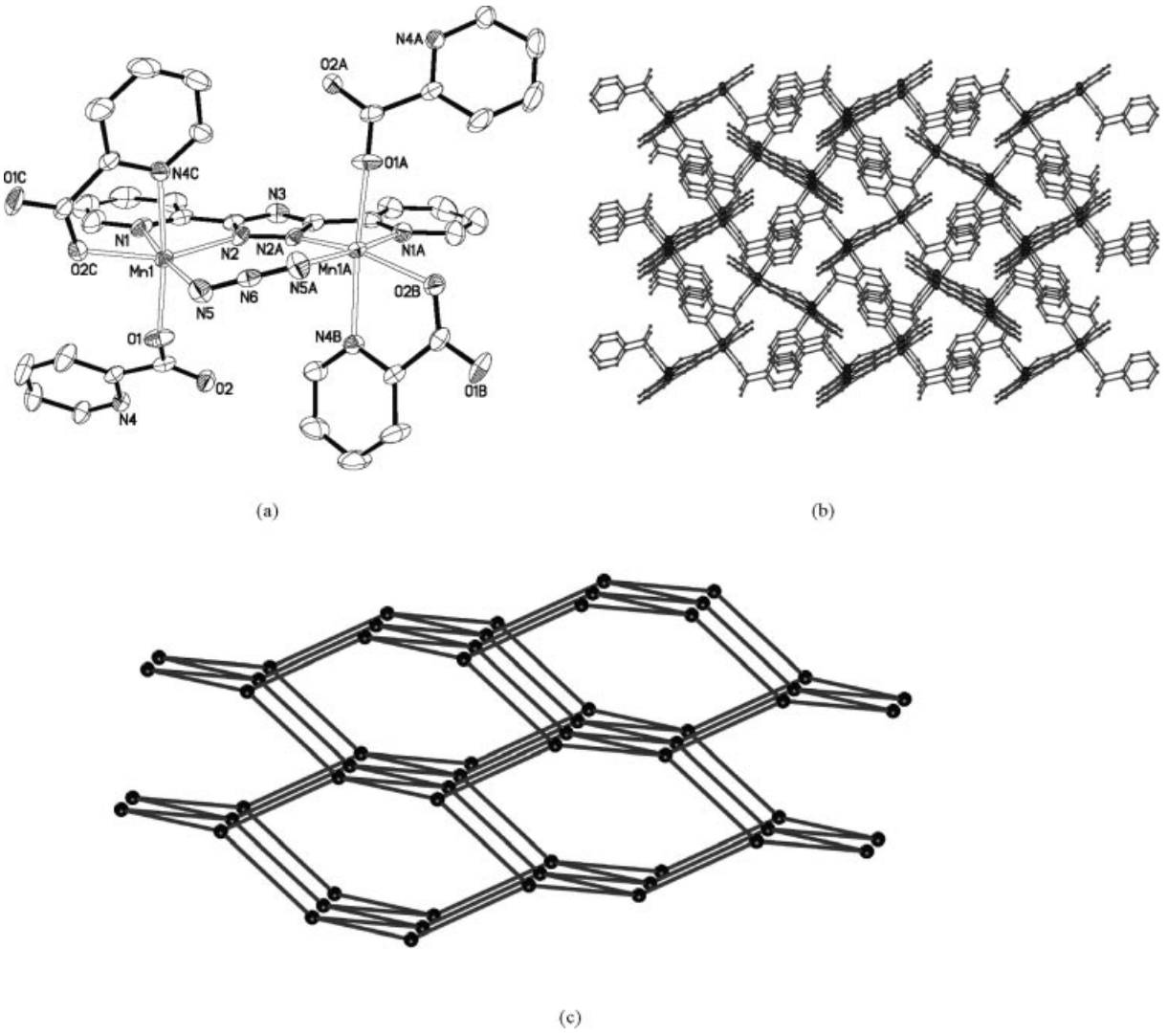

Figure 1. Views of the dinuclear SBU (a) (symmetry codes, A: $-x$, $1-y$, z; B: $-1/4-x$, $1/4+y$, $-1/4+z$; C: $1/4+x$, $3/4-y$, $-1/4+z$), the 3D structure (b), and the topology (each ball represents a Mn_2 SBU) (c) of **1**.

displays a sharp decrease upon cooling to a minimum of 0.27 emu K mol^{-1} at 7.2 K, and then a slight increase to a maximum of 0.51 emu K mol^{-1} at 5.7 K, finally decreasing again upon further cooling to 2 K.

The $\chi_M T$ value per Mn^{II} of ca. 3.82 emu K mol^{-1} at 300 K is slightly lower than the calculated value of 4.38 emu K mol^{-1} for magnetically isolated high-spin Mn^{II} ions ($S = 5/2$, $g = 2.0$). The temperature dependence of magnetic susceptibility above 100 K obeys the Curie–Weiss law $\chi_M = C/(T - \theta)$ with a Weiss constant $\theta = -70.0(6)$ K and a Curie constant $C = 4.73(1)$ cm^3 mol^{-1} K, indicating a dominant AF interaction between the metal centers (Figure 4, inset). Therefore, we can assume an AF coupling between the dimetallic centers via the EE-azide and *cis*-bpt bridges, probably together with a weak AF coupling between the dimeric SBUs in the 3D structure via the *syn-anti* carboxylate bridge. These are in agreement with the observation of AF interactions for Mn^{II} complexes connected via EE-azide, *cis*-bpt,[21] or *syn-anti* carboxylate bridges.[22] The magnetic exchange between the Mn^{II} ions follows two pathways: intradimeric via EE-azide and *cis*-bpt, as well as interdimeric via *syn-anti* carboxylate bridges. The intradimeric interaction (J) can be expressed as: $\hat{H}_{ex} = -2J\hat{S}_1\hat{S}_2$. The susceptibility per Mn_2 (χ'_{dimer}) can be given as shown in Equation (1).[23]

$$\chi'_{dimer} = \frac{2N\beta^2 g^2}{kT}\left[\frac{55e^{30x} + 30e^{20x} + 14e^{12x} + 5e^{6x} + e^{2x}}{11e^{30x} + 9e^{20x} + 7e^{12x} + 5e^{6x} + 3e^{2x} + 1}\right] \quad (1)$$

Taking into consideration the possibility of the interactions between the dinuclear SBUs in the crystal lattice, a correction for the molecular field is made [Equation (2)].

$$\chi_M = \frac{\chi'_{dimer}}{1 - 2zJ'\chi'_{dimer}/N\beta^2 g^2} \quad (2)$$

Where N is the Avogadro number, β is the Bohr magneton, k is the Boltzmann constant, $x = J/kT$, J is the intra-

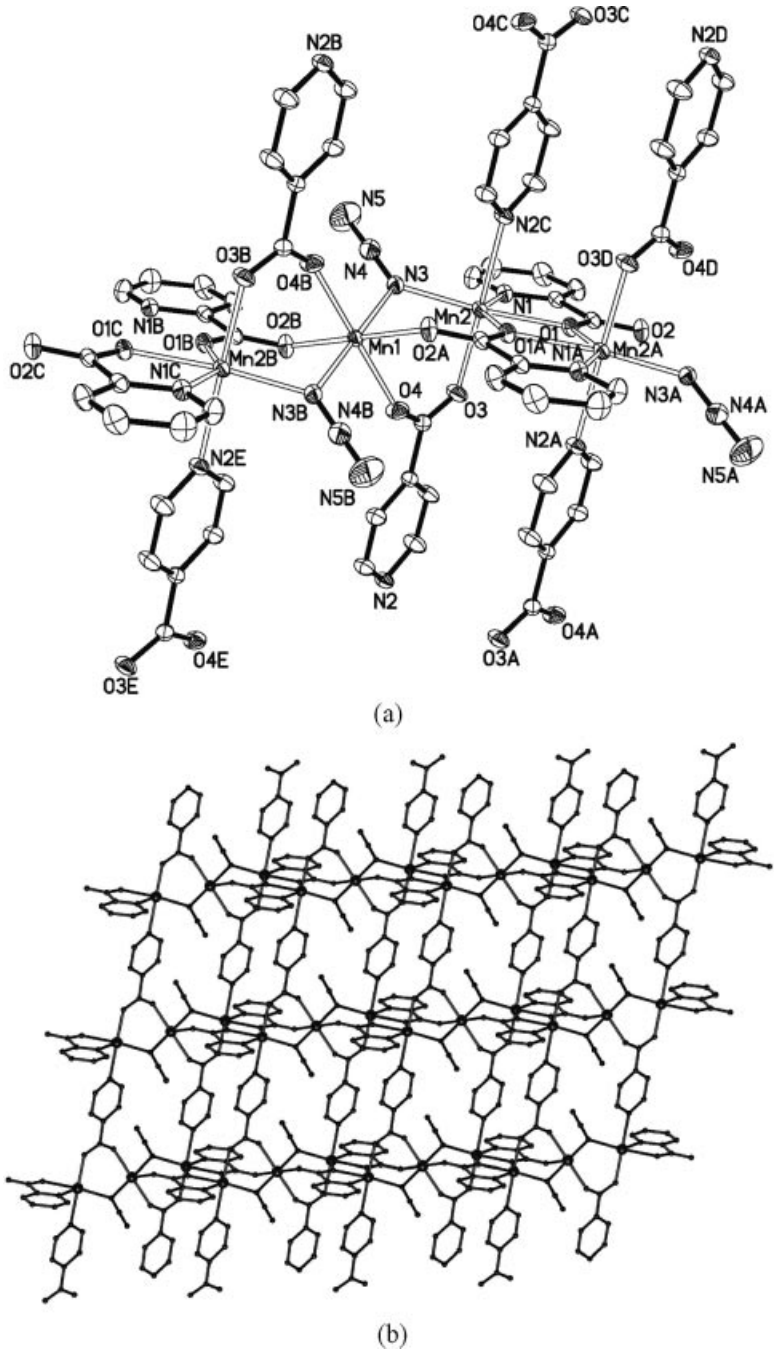

Figure 2. Views of the SBU (a) (symmetry codes, A: $-x, -y, -z$; B: $1-x, -y, -z$; C: $1+x, y, z$; D: $x, 1+y, z$; E: $-x, -1-y, -z$; F: $1-x, -1-y, -z$) and the 2D structure viewed along the c axis (b) in **2**.

dimer coupling constant, J' is the interdimer exchange interaction, and z is the number of nearest neighbors of the dimer. The best fitting of the experimental magnetic data above 40 K to Equation 2 gives the following parameters: $g = 2.04(1)$, $J = -3.71(2)\ cm^{-1}$, $zJ' = -1.35(3)\ cm^{-1}$ and $R = 6.95\times10^{-7}$, where $R = \Sigma[(\chi_M T)_{obs} - (\chi_M T)_{calcd}]^2/\Sigma[(\chi_M T)_{obs}]^2$. The results are in good agreement with those reported for 2D Mn^{II} complexes containing EE azide bridging networks [19,24] and confirm that the interactions mediated via the EE-azide and *cis*-bpt, and *syn-anti* carboxylate bridges are all AF interactions. However, it should be noted that the fitted values for J and zJ' are only qualitatively valid, because their comparability in magnitude does not meet the requirement of the molecular field approximation that zJ' should be much smaller than J.[24]

The magnetic properties of **1** in the low-temperature region are more complicated: the susceptibility exhibits first an increase, then a decrease, and finally a rapid increase. Though the intradimer and interdimer AF interactions tend to align the Mn^{II} spins in a compensated way to give a zero

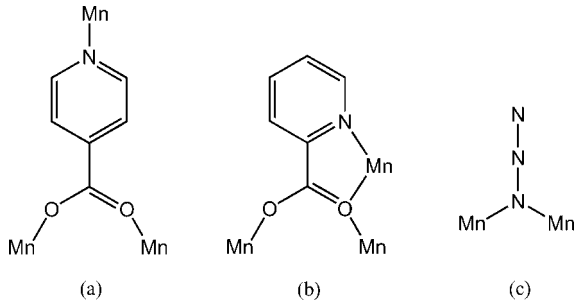

Figure 3. Coordination modes of ina (a), pa (b), and azide (c) in **2**.

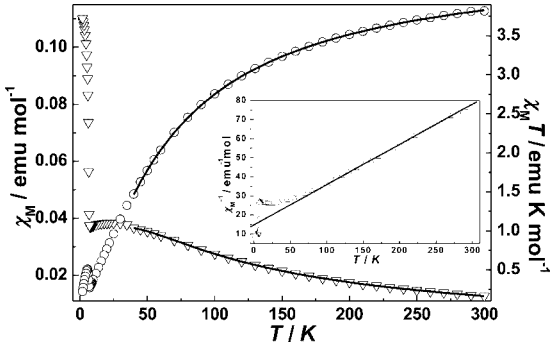

Figure 4. Temperature dependence of χ_M (▽) and $\chi_M T$ (○) for **1**. The dots are experimental values and the solid lines represent the best fits. Inset: temperature dependence of χ_M^{-1} (Δ) for **1**; the solid line represents the best fit of the Curie–Weiss law $\chi_M = C/(T - \theta)$.

residual moment, the low-temperature magnetic behavior of **1**, in which both χ_M and $\chi_M T$ increase sharply, suggests the existence of uncompensated residual spin moments and the occurrence of long-range weak F ordering.[25] The weak ferromagnetism may come from spin canting: the antiferromagnetically coupled local spins are not perfectly antiparallel but canted to each other, resulting in uncompensated residual spins.[19,24] The correlation between the residual spins may lead to long-range ordering. In **1**, the $\chi_M T$ values increase rapidly upon cooling below 7 K, indicating an F-like correlation. To further observe the magnetic transition at low temperature, FC (field-cooled) and ZFC (zero-field-cooled) magnetization measurements were carried out at 100 G below 30 K. As depicted in Figure 5a, compound **1** displays weak spontaneous magnetization that can be attributed to the onset of long-range ordering of the canted spins. The divergence of the ZFC and FC data below T_c = 6.5 K indicates irreversibility arising from the formation of an ordered magnetic state. To confirm this phenomenon, FC magnetizations at different fields were applied, as the magnetic behavior of a weak ferromagnetism arising from spin canting is rather field-dependent. As expected, the field dependence of the FC magnetization was really observed (Figure 5b). The increase in the χ_M and $\chi_M T$ values become imperceptible at higher fields at the measured temperature, and these curves show no rise anymore at a magnetic field of 20 kG or above, indicating that the weak 3D AF interaction is overcome by the external field to result in an ordered F phase.

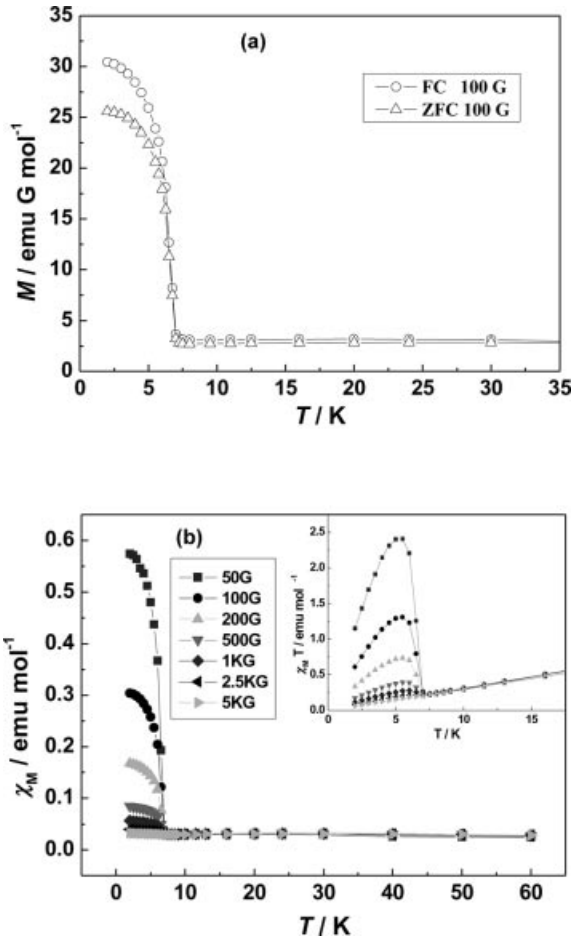

Figure 5. FC and ZFC magnetization plots at 100 G (a) and FC magnetizations in the forms of χ_M and $\chi_M T$ (inset) vs. T plots at different fields (b) for **1**.

Further experimental evidence for the spin-canted weak ferromagnetism in **1** comes from field-dependent isothermal magnetization measurements at 2 K (Figure 6). In the high-field region ($H > 15$ kG), the magnetization increases linearly with the field, and the magnetization value (0.364 Nβ) at the highest field (70 kG) is far below the saturation value (5 Nβ) expected for Mn^{II} species (S = 5/2). This behavior is consistent with weak ferromagnetism due to spin canting.[25] A hysteresis loop was observed at 2 K with a remnant magnetization (M_r) of 0.005 Nβ and a coercive field (H_c) of 820 G (Figure 6, inset), confirming the weak F ordering at low temperature.

It is well-known that spin canting may arise from single-ion magnetic anisotropy and/or antisymmetric exchange (Dzyaloshinsky–Moriya interaction).[26,27] Considering the isotropic character of the Mn^{II} ion, it has been often suggested that the Dzyaloshinsky–Moriya interaction is the main source of spin canting in Mn^{II} compounds,[27,28] which is consistent with the acentric *Fdd2* space group of **1**. This may suggest that spin canting has a significant contribution from acentric symmetry between the interacting spin centers.

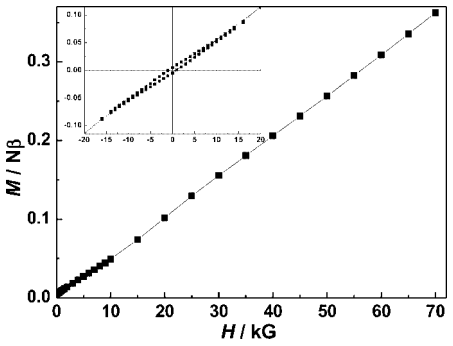

Figure 6. Field dependence of magnetization of **1** at 2 K. Inset: The hysteresis loop at 2 K.

Magnetic Properties of 2

The $\chi_M T$ vs. T plot for compound **2** is shown in Figure 7. The $\chi_M T$ value (4.01 emu K mol^{-1}) per Mn^{II} at 300 K is somewhat lower than that expected for a high-spin Mn^{II} ion (4.38 emu K mol^{-1}). The magnetic susceptibility above 50 K obeys the Curie–Weiss law with a Weiss constant, θ = –45.1(3) K, and a Curie constant, C = 4.63(1) cm^3 mol^{-1} K, indicating the presence of a dominant AF interaction (Figure 7, inset). On cooling, $\chi_M T$ falls to 1.67 emu K mol^{-1} at 14 K and then rises at lower temperatures to reach a maximum value of 3.49 emu K mol^{-1} at 2 K. This behavior is the typical of ferrimagnetism.

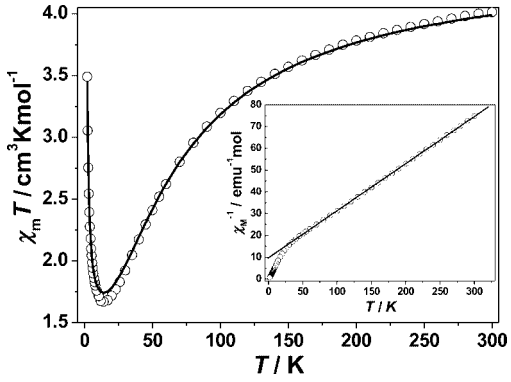

Figure 7. Plot of $\chi_M T$ vs. T for **2**; the solid line represents the best fit of the data according to the theoretical model. Inset: temperature dependence of χ_M^{-1} for **2**; the solid line represents the best fit of the Curie–Weiss law $\chi_M = C/(T - \theta)$.

The ferrimagnetic behavior of **2** can be suggested to arise from intrachain magnetic interactions due to the fact that the Mn^{II} chains are well separated by the ina bridges, in agreement with the absence of peaks in the real parts, χ', above 2 K in the curves of ac susceptibility (Figure S1). There are two kinds of magnetic exchange pathways in compound **2** with a $J_1J_1J_2$ repeating sequence according to the chain topology: one consists of two *syn-syn* μ_2-1,3-carboxylate bridges and an EO azide bridge; the other consists of two $\mu_{1,1}$-O bridges from two μ_3-carboxylate groups (Figure 8a). Due to noncompensation in spin moments within such a chain, the magnetic exchange through the former kind of bridges should be AF and that through the latter must be F. The exchanges alternate according to an AF-AF-F repeating sequence to produce the spin topology that corresponds to a (5, 5/2) ferromagnetic chain (Figure 8b). The field-dependent magnetization curve at 2 K indicates that the saturation magnetization per Mn^{II} atom, achieved at 70 kG, is ca. 1.73 Nβ (Figure 9). This value is consistent with an S = 5/2 spin state per $[Mn_3(ina)_2(pa)_2(N_3)_2]$ basic unit, indicating that the Mn^{II} chain is a typical (5, 5/2) topological ferrimagnetic chain with alternating AF-AF-F interaction.[25,29–31]

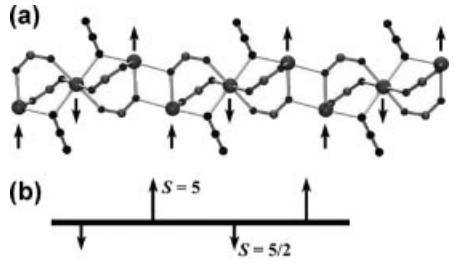

Figure 8. Bridging chain (a) and spin topology of the (5, 5/2) ferrimagnetic chain (b) in **2**.

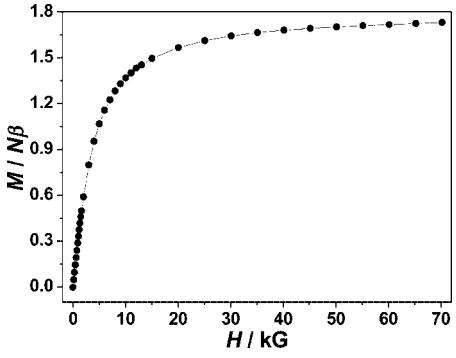

Figure 9. The field-dependent magnetization curve of **2** at 2 K.

To evaluate the exchanges, a nonlinear least-squares fitting of the theoretical expression proposed by Escuer et al.[31a,31b] to the experimental data has been performed by varying g, J_1, J_2 and minimizing the residual $R = [\Sigma(\chi_{obs}T - \chi_{calc}T)^2/\Sigma(\chi_{obs}T)^2]$. The best fit to the data above 2 K is achieved with g = 2.02(1), J_1 = –6.21(8) cm^{-1}, J_2 = 0.22(1) cm^{-1}, $R = 1.10 \times 10^{-4}$. The J_1 value is associated with the AF exchange through the mixed carboxylate/azide (EO) bridges, in agreement with the previous observations in Mn^{II} complexes,[8c,32] whereas the double $\mu_{1,1}$-O bridges mediate a ferromagnetic (J_2) interaction, which may arise from accidental orthogonality between magnetic orbitals around the metal ions.[29,33] Relative to the 3D complex of trinuclear SBUs $[Mn_3(4\text{-aba})_6]_n$ (J_1 = –4.5 cm^{-1}, J_2 = 0.38 cm^{-1}),[29] the AF is slightly stronger, while the F is slightly weaker, which may be attributed to the fact that $\mu_{1,1}$-azide bridges transmit stronger AF interactions with a large Mn1–N3–Mn2 angle [109.86(8)°], while $\mu_{1,1}$-O bridges transmit a weaker F exchange as the Mn2–O1–Mn2A angle [105.56(6)°] is larger than that in $[Mn_3(4\text{-aba})_6]_n$ (97.10°).

Conclusions

Two manganese(II) coordination polymers, $[Mn_2(bpt)(pa)_2(N_3)]_n$ (**1**) and $[Mn_3(ina)_2(pa)_2(N_3)_2]_n$ (**2**), have been synthesized under solvothermal conditions. The bpt and pa ligands were generated in situ by cyclocondensation and hydrolysis of 2-pyridylamidrazone, respectively. Magnetic studies show that **1**, featuring a diamondoid network, exhibits spin-canting magnetism due to the lack of inversion centers between the interacting spin centers, while **2** shows a topological ferrimagnetic behavior in an AF-AF-F sequence, in which the magnetic exchanges through the mixed $\mu_{1,3}$-carboxylate/$\mu_{1,1}$-azide bridges and the double $\mu_{1,1}$-carboxylate bridges are AF and F, respectively.

Experimental Section

General Remarks: The reagents and solvents employed were commercially available and used as received without further purification. The C, H, and N microanalyses were carried out with a Vario EL elemental analyzer. The FTIR spectra were recorded from KBr pellets in the range 400–4000 cm^{-1} with a Bruker TENSOR 27 FTIR spectrometer. Magnetic susceptibility data of powder samples were collected in the temperature range 2–300 K with the use of a Quantum Design MPMS XL-7 SQUID magnetometer. The diamagnetic corrections were estimated from the Pascal's constants. 2-Pyridylamidrazone,[34] $MnC_2O_4{\cdot}3H_2O$,[17] and $Mn(ina)_2{\cdot}0.5EtOH{\cdot}0.5H_2O$[18] were synthesized according to the published procedures, and their identities were confirmed with NMR spectra or elemental analysis.

Synthesis of $[Mn_2(bpt)(pa)_2(N_3)]_n$ (1): A mixture of 2-pyridylamidrazone (0.272 g, 2 mmol), $MnC_2O_4{\cdot}3H_2O$ (0.197 g, 1 mmol), NaN_3 (0.130 g, 2 mmol), and 95% C_2H_5OH (4 mL) was heated in a 15-mL Teflon-lined autoclave at 120 °C for 3 d, followed by slow cooling (5 °C h^{-1}) to room temperature. After the mixture was filtered and washed with 95% ethanol, yellow block crystals were collected and dried in air (0.247 g, yield ca. 80% based on Mn). $C_{24}H_{16}Mn_2N_{10}O_4$ (618.34): C 46.62, H 2.61, N 22.65; found C 46.62, H 2.65, N 22.66. FTIR: $\tilde{\nu}$ = 3852 (w), 3745 (w), 3387 (vs), 3077 (w), 2061 (s), 1575 (s), 1463 (m), 1389 (vs), 1145 (m), 1092 (m), 1043 (m), 848 (w), 806 (w), 759 (m), 700 (m), 637 (m), 528 (m) cm^{-1}.

Synthesis of $[Mn_3(ina)_2(pa)_2(N_3)_2]_n$ (2): The reaction was carried out by a method similar to that for **1**, using $Mn(ina)_2{\cdot}0.5EtOH{\cdot}0.5H_2O$ (0.331 g, 1 mmol) instead of $MnC_2O_4{\cdot}3H_2O$. After the mixture was filtered and washed with 95% ethanol, yellow block crystals were collected and dried in air (0.181 g, yield ca. 74% based on Mn). $C_{24}H_{16}Mn_3N_{10}O_8$ (737.28): C 39.10, H 2.19, N 19.00; found C 39.07, H 2.21, N 18.86. FTIR: $\tilde{\nu}$ = 3745 (w), 3393 (m), 3348 (m), 3068 (w), 2979 (w), 2622 (w), 2001 (s), 1620 (s), 1550 (vs), 1475 (m), 1395 (s), 1336 (m), 1292 (m), 1171 (w), 1092 (w), 1050 (m), 1010 (m), 850 (m), 770 (m), 698 (vs), 648 (w), 603 (w), 556 (w), 451 (m) cm^{-1}.

X-ray Crystallographic Study: Diffraction intensities for the compounds were collected at 293(2) K with a Bruker Apex CCD area-detector diffractometer (Mo-K_α, λ = 0.71073 Å). Absorption corrections were applied by using the multiscan program SADABS.[35] The structures were solved with direct methods and refined with the full-matrix least-squares technique using the SHELXTL program package.[36] Anisotropic thermal parameters were applied to all the non-hydrogen atoms. The organic hydrogen atoms were generated geometrically (C–H: 0.96 Å). The absolute structure of **1** has been determined with a Flack parameter of 0.01(3).[37] Crystal data as well as details of data collection and refinement for the com-

Table 1. Crystallographic data and structure refinement for **1** and **2**.

Complex	**1**	**2**
Molecular formula	$C_{24}H_{16}Mn_2N_{10}O_4$	$C_{24}H_{16}Mn_3N_{10}O_8$
Formula weight	618.34	737.28
Crystal system	orthorhombic	triclinic
Space group	*Fdd*2	$P\bar{1}$
a/Å	19.549(3)	8.8369(6)
b/Å	27.242(4)	9.5269(6)
c/Å	9.6170(13)	9.9558(7)
α/°	90	105.425(1)
β/°	90	107.066(1)
γ/°	90	106.808(1)
V/Å^3	5121.6(12)	708.42(8)
Z	8	1
$\rho_{calcd.}$/g cm^{-3}	1.604	1.728
μ/mm^{-1}	1.039	1.384
Reflections collected	4666	5749
Independent reflections	2584	2926
Data/restraints/parameters	2216/0/182	2683/0/205
R indices $[I > 2\sigma(I)]$[a], *wR2*[b] (all data)	0.0558, 0.1042	0.0280, 0.0777
$(\Delta\rho_{max}/\Delta\rho_{min})$/e Å^{-3}	0.54/–0.36	0.39/–0.22

[a] $R_1 = \Sigma||F_o| - |F_c||/\Sigma|F_o|$. [b] $wR_2 = [\Sigma w(F_o^2 - F_c^2)^2/\Sigma w(F_o^2)^2]^{1/2}$.

Table 2. Selected bond lengths [Å] and bond angles [°] of **1** and **2**.[a]

1			
Mn1–O1	2.114(3)	Mn1–N1	2.301(4)
Mn1–N2	2.222(4)	Mn1–N5	2.198(4)
Mn1–O2C	2.166(4)	Mn1–N4C	2.283(4)
O1–Mn1–N1	87.7(1)	O1–Mn1–N2	96.1(1)
O1–Mn1–N5	92.3(2)	O1–Mn1–O2C	99.4(1)
O1–Mn1–N4C	173.2(1)	N1–Mn1–N2	73.3(1)
N1–Mn1–N5	172.1(2)	N1–Mn1–N4C	94.5(11)
N2–Mn1–N4C	90.8(1)	N2–Mn1–N5	98.8(1)
O2C–Mn1–N2	158.7(1)	O2C–Mn1–N1	92.7(1)
O2C–Mn1–N5	95.1(2)	O2C–Mn1–N4C	74.1(1)
N4C–Mn1–N5	86.3(2)	Mn1–N5–N6	119.0(3)
2			
Mn1–O2A	2.207(1)	Mn1–O4	2.125(2)
Mn1–N3	2.227(2)	Mn2–O1	2.216(2)
Mn2–N3	2.133(2)	Mn2–N1	2.257(2)
Mn2–O3	2.168(2)	Mn2–N2D	2.357(2)
O4–Mn1–N3	89.30(7)	O2C–Mn1–O4	91.74(7)
O2A–Mn1–O4	88.26(7)	O2C–Mn1–N3	84.77(6)
O4–Mn1–N3B	90.70(7)	O4B–Mn1–N3	90.70(7)
O2A–Mn1–N3	95.23(6)	O2C–Mn1–N3B	95.23(6)
O2C–Mn1–O4B	88.26(7)	O2A–Mn1–N3B	84.77(6)
O2A–Mn1–O4B	91.74(7)	O1–Mn2–O3	93.46(6)
O4B–Mn1–N3B	89.30(7)	O1–Mn2–N3	171.85(7)
O1–Mn2–N1	72.86(6)	O1–Mn2–O1A	74.44(5)
O1–Mn2–N2D	87.44(6)	O3–Mn2–N3	93.31(7)
O3–Mn2–N1	89.86(7)	O1A–Mn2–O3	94.71(6)
O3–Mn2–N2D	177.78(6)	N1–Mn2–N2D	88.46(7)
N1–Mn2–N3	111.69(7)	N2D–Mn2–N3	85.95(7)
O1A–Mn2–N1	147.18(7)	O1A–Mn2–N2D	87.49(6)
O1A–Mn2–N3	100.48(6)	Mn1–N3–N4	121.30(18)
Mn2–O1–Mn2A	105.56(6)	Mn1–N3–Mn2	109.86(8)

[a] Symmetry codes for **1**: C: 1/4 + *x*, 3/4 – *y*, –1/4 + *z*. For **2**: A: –*x*, –*y*, –*z*; B: 1 – *x*, –*y*, –*z*; D: *x*, 1 + *y*, *z*.

plexes are summarized in Table 1. Selected bond lengths and bond angles are listed in Table 2.

CCDC 624799–624800 contain the supplementary crystallographic data for this paper. These data can be obtained free of charge via www.ccdc.cam.ac.uk/conts/retrieving.html (or from the Cambridge Crystallographic Data Centre, 12 Union Road, Cambridge CB21EZ, UK; Fax: +44-1223-336-033).

Supporting Information (see footnote on the first page of this article): Temperature dependence of the real χ' and imaginary χ'' parts of the ac susceptibility (H_{dc} = 0 Oe, H_{ac} = 3 Oe) for **1**.

Acknowledgments

This work was supported by the National Natural Science Foundation of China (No. 20531070) and the Science and Technology Department of Guangdong Province (No. 04205405).

[1] O. Kahn, *Molecular Magnetism*, VCH, Weinheim, Germany, **1993**.

[2] a) O. Kahn, *Acc. Chem. Res.* **2000**, *33*, 647–657; b) J. S. Miller, J. L. Manson, *Acc. Chem. Res.* **2001**, *34*, 563–570; c) M. Sakamoto, K. Manseki, H. Ökawa, *Coord. Chem. Rev.* **2001**, *219–221*, 379–414; d) C. Benelli, D. Gatteschi, *Chem. Rev.* **2002**, *102*, 2369–2388; e) I. Ciofini, C. A. Daul, *Coord. Chem. Rev.* **2003**, *238–239*, 187–209.

[3] a) A. L. Barra, A. Caneschi, A. Cornia, F. Fabrizi de Biani, D. Gatteschi, C. Sangregorio, R. Sessoli, L. Sorace, *J. Am. Chem. Soc.* **1999**, *121*, 5302–5310; b) D. Gatteschi, R. Sessoli, *Angew. Chem. Int. Ed.* **2003**, *42*, 268–297; c) R. H. Laye, E. J. L. McInnes, *Eur. J. Inorg. Chem.* **2004**, 2811–2818; d) E. K. Brechin, *Chem. Commun.* **2005**, 5141–5153; e) N. T. Madhu, J.-K. Tang, I. J. Hewitt, R. Clerac, W. Wernsdorfer, J. van Slageren, C. E. Anson, A. K. Powell, *Polyhedron* **2005**, *24*, 2864–2869.

[4] a) Y.-Z. Zheng, M.-L. Tong, W.-X. Zhang, X.-M. Chen, *Angew. Chem. Int. Ed.* **2006**, *45*, 6310–6314; b) Y.-Z. Zheng, M.-L. Tong, W.-X. Zhang, X.-M. Chen, *Chem. Commun.* **2006**, 165–167; c) X.-N. Cheng, W.-X. Zhang, Y.-Z. Zheng, X.-M. Chen, *Chem. Commun.* **2006**, 3603–3605; d) M.-H. Zeng, B. Wang, X.-Y. Wang, W.-X. Zhang, X.-M. Chen, S. Gao, *Inorg. Chem.* **2006**, *45*, 7069–7076; e) M.-H. Zeng, W.-X. Zhang, X.-Z. Sun, X.-M. Chen, *Angew. Chem. Int. Ed.* **2005**, *44*, 3079–3082; f) S. Xiang, X.-T. Wu, J.-J. Zhang, R.-B. Fu, S.-M. Hu, X.-D. Zhang, *J. Am. Chem. Soc.* **2005**, *127*, 16352–16353.

[5] a) E. Ruiz, J. Cano, S. Alvarez, P. Alemany, *J. Am. Chem. Soc.* **1998**, *120*, 11122–11129; b) M. A. M. Abu-Youssef, A. Escuer, D. Gatteschi, M. A. S. Goher, F. A. Mautner, R. Vicente, *Inorg. Chem.* **1999**, *38*, 5716–5723; c) J. L. Manson, A. M. Arif, J. S. Miller, *Chem. Commun.* **1999**, 1479–1480; d) S.-B. Wang, G.-M. Yang, D.-Z. Liao, L.-C. Li, *Inorg. Chem.* **2004**, *43*, 852–854; e) C.-M. Liu, S. Gao, D.-Q. Zhang, Y.-H. Huang, R.-G. Xiong, Z.-L. Liu, F.-C. Jiang, D.-B. Zhu, *Angew. Chem. Int. Ed.* **2004**, *43*, 990–994; f) J. Cano, Y. Journaux, M. A. S. Goher, M. A. M. Abu-Youssef, F. A. Mautner, G. J. Reiß, A. Escuer, R. Vicente, *New J. Chem.* **2005**, *29*, 306–314; g) Y.-Z. Zhang, H.-Y. Wei, F. Pan, Z.-M. Wang, Z.-D. Chen, S. Gao, *Angew. Chem. Int. Ed.* **2005**, *44*, 5841–5846; h) T. Liu, Y.-J. Zhang, Z.-M. Wang, S. Gao, *Inorg. Chem.* **2006**, *45*, 2782–2784; i) X.-Y. Wang, L. Wang, Z.-M. Wang, S. Gao, *J. Am. Chem. Soc.* **2006**, *128*, 674–675; j) C.-H. Ge, A.-L. Cui, Z.-H. Ni, Y.-B. Jiang, L.-F. Zhang, J. Ribas, H.-Z. Kou, *Inorg. Chem.* **2006**, *45*, 4883–4885.

[6] a) S. S. Tandon, L. K. Thompson, M. E. Manuel, J. N. Bridson, *Inorg. Chem.* **1994**, *33*, 5555–5570; b) L. K. Thompson, S. S. Tandon, M. E. Manuel, *Inorg. Chem.* **1995**, *34*, 2356–2366.

[7] a) Y.-H. Liu, H.-L. Tsai, Y.-L. Lu, Y.-S. Wen, J.-C. Wang, K.-L. Lu, *Inorg. Chem.* **2001**, *40*, 6426–6431; b) R.-G. Xiong, Y.-R. Xie, C.-M. Che, *J. Chem. Soc., Dalton Trans.* **2001**, 777–779.

[8] a) M. A. S. Goher, M. A. M. Abu-Youssef, F. A. Mautner, A. Popitsch, *Polyhedron* **1992**, *11*, 2137–2141; b) A. Escuer, R. Vicente, F. A. Mautner, M. A. S. Goher, *Inorg. Chem.* **1997**, *36*, 1233–1236; c) H.-J. Chen, Z.-W. Mao, S. Gao, X.-M. Chen, *Chem. Commun.* **2001**, 2320–2321; d) F.-C. Liu, Y.-F. Zeng, J.-R. Li, X.-H. Bu, H.-J. Zhang, J. Ribas, *Inorg. Chem.* **2005**, *44*, 7298–7300; e) F.-C. Liu, Y.-F. Zeng, J. Jiao, X.-H. Bu, J. Ribas, S.-R. Batten, *Inorg. Chem.* **2006**, *45*, 2776–2778; f) F.-C. Liu, Y.-F. Zeng, J. Jiao, J.-R. Li, X.-H. Bu, J. Ribas, S.-R. Batten, *Inorg. Chem.* **2006**, *45*, 6129–6131; g) Y.-F. Zeng, F.-C. Liu, J.-P. Zhao, S. Cai, X.-H. Bu, J. Ribas, *Chem. Commun.* **2006**, 2227–2229; h) Z. He, Z.-M. Wang, S. Gao, C.-H. Yan, *Inorg. Chem.* **2006**, *45*, 6694–6705.

[9] a) S.-H. Feng, R.-R. Xu, *Acc. Chem. Res.* **2001**, *34*, 239–247; b) C. S. Cundy, P. A. Cox, *Chem. Rev.* **2003**, *103*, 663–702.

[10] a) O. R. Evans, W.-B. Lin, *Acc. Chem. Res.* **2002**, *35*, 511–522; b) J.-Y. Lu, *Coord. Chem. Rev.* **2003**, *246*, 327–347.

[11] a) X.-M. Zhang, *Coord. Chem. Rev.* **2005**, *249*, 1201–1219; b) X.-M. Chen, M.-L. Tong, *Acc. Chem. Res.* **2007**, *40*, 162–170.

[12] a) R.-G. Xiong, X. Xue, H. Zhao, X.-Z. You, B. F. Abrahams, Z.-L. Xue, *Angew. Chem. Int. Ed.* **2002**, *41*, 3800–3803; b) C.-M. Liu, S. Gao, H.-Z. Kou, *Chem. Commun.* **2001**, 1670–1671; c) R.-H. Wang, M.-C. Hong, J.-H. Luo, R. Cao, J.-B. Weng, *Chem. Commun.* **2003**, 1018–1019.

[13] a) X.-M. Zhang, M.-L. Tong, X.-M. Chen, *Angew. Chem. Int. Ed.* **2002**, *41*, 1029–1031; b) J. Tao, Y. Zhang, M.-L. Tong, X.-M. Chen, T. Yuen, C.-L. Lin, X.-Y. Huang, J. Li, *Chem. Commun.* **2002**, *13*, 1342–1343; c) J.-P. Zhang, S.-L. Zheng, X.-C. Huang, X.-M. Chen, *Angew. Chem. Int. Ed.* **2004**, *43*, 206–209; d) J.-P. Zhang, Y.-Y. Lin, X.-C. Huang, X.-M. Chen, *J. Am. Chem. Soc.* **2005**, *127*, 5495–5506; e) Y.-Z. Zheng, M.-L. Tong, X.-M. Chen, *New J. Chem.* **2004**, *28*, 1412–1415; f) Y.-T. Wang, M.-L. Tong, H.-H. Fan, H.-Z. Wang, X.-M. Chen, *Dalton Trans.* **2005**, 424–426.

[14] L. Cheng, W.-X. Zhang, B.-H. Ye, J.-B. Lin, X.-M. Chen, *Inorg. Chem.* **2007**, *46*, 1135–1143.

[15] A. S. Shawali, A. Osman, H. H. Hassaneen, *Indian J. Chem.* **1972**, *10*, 965–967.

[16] X.-Y. Wang, L. Gan, S.-W. Zhang, S. Gao, *Inorg. Chem.* **2004**, *43*, 4615–4625.

[17] W.-Y. Wu, Y. Song, Y.-Z. Li, X.-Z. You, *Inorg. Chem. Commun.* **2005**, *8*, 732–736.

[18] Q. Wei, M. Nieuwenhuyzen, S. L. James, *Microporous Mesoporous Mater.* **2004**, *73*, 97–100.

[19] E.-Q. Gao, Y.-F. Yue, S.-Q. Bai, Z. He, S.-W. Zhang, C.-H. Yan, *Chem. Mater.* **2004**, *16*, 1590–1596.

[20] a) R. L. Rardin, P. Poganiuch, A. Bino, D. P. Goldberg, W. B. Tolman, S. Liu, S. J. Lippard, *J. Am. Chem. Soc.* **1992**, *114*, 5240–5249; b) V. Tangoulis, D. A. Malamatari, K. Soulti, V. Stergiou, C. P. Raptopoulou, A. Terzis, T. A. Kabanos, D. P. Kessissoglou, *Inorg. Chem.* **1996**, *35*, 4974–4983; c) G. Fernández, M. Corbella, J. Mahía, M. A. Maestro, *Eur. J. Inorg. Chem.* **2002**, 2502–2510.

[21] R. P. Paul, J. M. W. L. Birker, J. G. Haasnoot, G. C. Verschoor, J. Reedijk, *Inorg. Chem.* **1985**, *24*, 4128–4133.

[22] a) X.-M. Chen, Y.-X. Tong, Z.-T. Xu, T. C. W. Mak, *J. Chem. Soc., Dalton Trans.* **1995**, 4001–4004; b) H. Iikura, T. Nagata, *Inorg. Chem.* **1998**, *37*, 4702–4711; c) W. Zhao, Y. Song, T. Okamura, J. Fan, W.-Y. Sun, N. Ueyama, *Inorg. Chem.* **2005**, *44*, 3330–3336.

[23] a) M. E. Fisher, *Am. J. Phys.* **1964**, *32*, 343–346; b) C. J. O'Connor, *Prog. Inorg. Chem.* **1982**, *29*, 203–283.

[24] E.-Q. Gao, A.-L. Cheng, Y.-X. Xu, M.-Y. He, C.-H. Yan, *Inorg. Chem.* **2005**, *44*, 8822–8835.

[25] E.-Q. Gao, Y.-F. Yue, S.-Q. Bai, Z. He, C.-H. Yan, *J. Am. Chem. Soc.* **2004**, *126*, 1419–1429.

[26] a) I. E. Dzyaloshinsky, *Phys. Chem. Solids* **1958**, *4*, 241–255; b) T. Moriya, *Phys. Rev.* **1960**, *120*, 91–98.

[27] a) R. L. Carlin, *Magnetochemistry*, Springer-Verlag, Berlin, **1986**, pp. 148–154; b) S. R. Batten, P. Jensen, C. J. Kepert, M. Kurmoo, B. Moubaraki, K. S. Murray, D. J. Price, *J. Chem. Soc., Dalton Trans.* **1999**, 2987–2997; c) S. G. Carling, P. Day, D. Visser, R. K. Kremer, *J. Solid State Chem.* **1993**, *106*, 111–119.
[28] S. Han, J. L. Manson, J. Kim, J. S. Miller, *Inorg. Chem.* **2000**, *39*, 4182–4185.
[29] R.-H. Wang, E.-Q. Gao, M.-C. Hong, S. Gao, J.-H. Luo, Z.-Z. Lin, L. Han, R. Cao, *Inorg. Chem.* **2003**, *42*, 5486–5488.
[30] A. K. Ghosh, D. Ghoshal, E. Zangrando, J. Ribas, N. R. Chaudhuri, *Inorg. Chem.* **2005**, *44*, 1786–1793.
[31] a) M. A. M. Abu-Youssef, M. Drillon, A. Escuer, M. A. S. Goher, F. A. Mautner, R. Vicente, *Inorg. Chem.* **2000**, *39*, 5022–5027; b) A. Escuer, F. A. Mautner, M. A. S. Goher, M. A. M. Abu-Youssef, R. Vicente, *Chem. Commun.* **2005**, 605–606; c) M. A. M. Abu-Youssef, A. Escuer, A. S. G. Mohamed, F. A. Mautner, G. J. Reiß, R. Vicente, *Angew. Chem. Int. Ed.* **2000**, *39*, 1624–1626.
[32] L.-Y. Wang, Z.-L. Liu, C.-X. Zhang, Z.-Q. Liu, D.-Z. Liao, Z.-H. Jiang, S.-P. Yan, *Sci. China, Ser. B* **2003**, *46*, 533–537.
[33] W. E. Hatfield in *Magneto-Structural Correlations in Exchange Coupled Systems* (Eds.: R. D. Willet, D. Gatteschi, O. Kahn), Reidel, Dordrecht, **1984**, p. 555.
[34] F. H. Case, *J. Org. Chem.* **1965**, *30*, 931–933.
[35] G. M. Sheldrick, *SADABS 2.05*, University of Göttingen, **2002**.
[36] *SHELXTL 6.10*, Bruker Analytical Instrumentation, Madison, Wisconsin, USA, **2000**.
[37] H. D. Flack, *Acta Crystallogr., Sect. A* **1983**, *39*, 876–881.

Received: October 27, 2006
Published Online: April 23, 2007

